NANO LETTERS

2007
Vol. 7, No. 6
1542−1550

Elucidating the Mechanism of Cellular Uptake and Removal of Protein-Coated Gold Nanoparticles of Different Sizes and Shapes

B. Devika Chithrani[†,‡] and Warren C. W. Chan*[,†,‡,§]

Institute of Biomaterials and Biomedical Engineering, Materials Science and Engineering, Terrence Donnelly Center for Cellular and Biomolecular Research, University of Toronto, 160 College Street, 4th Floor, Toronto, Ontario M5S 3G9, Canada

Received February 14, 2007; Revised Manuscript Received March 26, 2007

ABSTRACT

We investigated the mechanism by which transferrin-coated gold nanoparticles (Au NP) of different sizes and shapes entered mammalian cells. We determined that transferrin-coated Au NP entered the cells via clathrin-mediated endocytosis pathway. The NPs exocytosed out of the cells in a linear relationship to size. This was different than the relationship between uptake and size. Furthermore, we developed a mathematical equation to predict the relationship of size versus exocytosis for different cell lines. These studies will provide guidelines for developing NPs for imaging and drug delivery applications, which will require "controlling" NP accumulation rate. These studies will also have implications in determining nanotoxicity.

The design of smart multifunctional nanosystems for intracellular imaging and targeted therapeutic applications requires a thorough understanding of the mechanisms of nanoparticles (NPs) entering and leaving the cells. For biological and clinical applications, the ability to control and manipulate the accumulation of NPs for an extended period of time inside a cell can lead to improvements in diagnostic sensitivity and therapeutic efficiency.[1,2] Furthermore, elucidating the exocytosis and metabolism of NPs in cells could lead to a better understanding of NP toxicity (i.e., if the NPs are trapped in vesicles and leave the cells intact, they are unlikely to induce cellular toxicity). Current studies in this research area have focused on coating biorecognition molecules on the surface of NPs to mediate cellular accumulation.[3,4] However, there is a lack of studies on the effect of a NP's physical dimension and geometry on cellular accumulation removal and kinetics.[5−7]

It has been demonstrated that size plays a role in cellular uptake of liposomes, polymer NPs, artificial viruses (DNA-coated glycocluster NPs), and inorganic nanostructures.[5,8−10] Aoyama and co-workers specifically investigated the effect of size and receptor contributions in glycoviral gene delivery, and they showed that the size of a glycovirus played an important role in its endocytosis-mediated transfection activities.[8] Fifty nm spherical viruses were identified as having the highest transfection activity. Viruses are not ideal candidates for such studies because of the difficulty in manipulating the size and shape of the same virus. Although not NPs, Mitragotri et al. showed that the shape of micrometer-sized particles mediated their uptake in alveolar macrophages.[11] Only recently, researchers have studied the relationship between both NP size and shape (of the same material composition) and its uptake kinetics and mechanism.[5] It was shown that NPs with a diameter of ∼50 nm were taken up by mammalian cells at a rate and concentration that was faster and higher, respectively, than other sizes and shapes.

In a previous paper,[5] we demonstrated the phenomenon that the quantitative uptake of gold NPs was heavily dependent upon size and shape. In this manuscript, we continued these studies to obtain a better understanding of the entire process. In comparison to the original paper, we investigated and captured the uptake process of the transferrin-coated NP entering cells by electron microscopy, established the mechanism of uptake, and quantitated the exocytosis process. We also provided simple equations and schematics to predict and explain this relationship. The results

* Corresponding author. E-mail: warren.chan@utoronto.ca.
† Institute of Biomaterials and Biomedical Engineering.
‡ Terrence Donnelly Center for Cellular and Biomolecular Research.
§ Materials Science and Engineering, Terrence Donnelly Center for Cellular and Biomolecular Research.

10.1021/nl070363y CCC: $37.00
Published on Web 04/28/2007

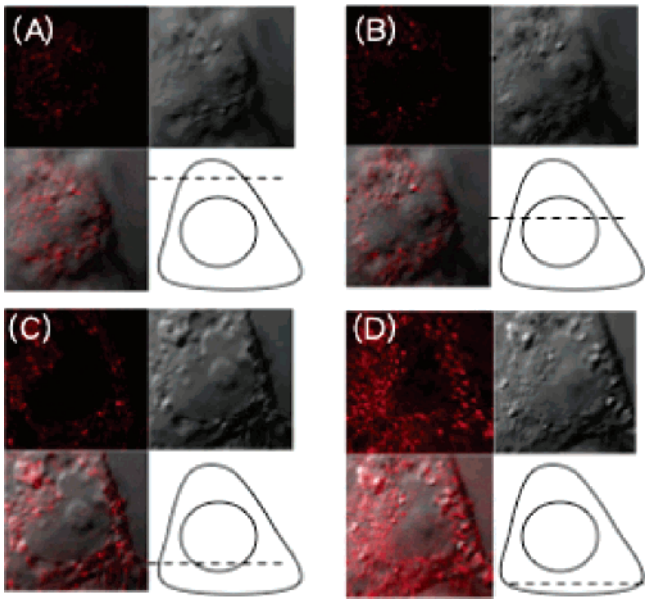

Figure 1. Confocal images at different *Z*-axis of transferrin-coated spherical gold nanoparticles conjugated with the organic fluorophore texas red. (A−D) Fluorescence images of cells with transferrin-coated gold nanoparticles and their corresponding DIC images. A schematic depicting the *Z*-axis of the image is shown with each of the four panels. Clearly, as the *Z*-axis moves from top to bottom of the Hela cell, we observed fluorescence spots throughout the Hela cell. If the transferrin-coated gold nanoparticles only bound onto the surface of the Hela cell, we would not observe fluorescence staining throughout the *Z*-axis. Coupling this data with TEM images indicates the transferrin-coated spherical gold nanoparticles did enter the Hela cell. Each cell is ∼15 μm.

from these studies will provide a better understanding in elucidating the mechanism and relationship of how size and shape of NP affect uptake, and in effect, these results would assist in the future design of nanostructures for biomedical applications. The results from these studies could be adapted toward understanding of how other NPs (coated with proteins) of different size and shape enters cells.

In this study, we used gold (Au) NPs as a model NP system because the size and shape of these NPs can be easily controlled during synthesis. They can also be quantified in biological samples using the techniques of inductively coupled plasma atomic emission spectroscopy (ICP-AES) and UV−visible spectrophotometry. For all studies, we coated the surface of the Au NPs with the protein transferrin, which carries iron into cells via the process of receptor-mediated endocytosis.[12−14] Transferrin has been extensively investigated as a potential ligand to enable drug targeting and delivery of therapeutic agents that would normally suffer from poor pharmacokinetic characteristics.[14,15−18] Transferrin was used as a model protein system. However, different proteins coated on the Au NPs may lead to different results. These studies on the transferrin-coated Au NPs of different size and shape could be used as a model for investigating other proteins coated on NPs. Therefore, the investigation of the cellular uptake and removal mechanism and dynamics of Au NPs-coated with transferrin will provide important information to the advancement of NPs for applications in drug delivery,[19−21] diagnostics,[22−25] and therapeutics.[26−28] Extensive investigation on other protein systems will be required before a complete understanding of how a NP's size and shape affect their cellular uptake and removal is obtained.

The uptake and removal of transferrin-coated spherical and rod-shaped Au NPs was carefully examined in three different cell lines (STO cells, which are fibroblast cells, HeLa cells, which are ovarian cancer cells, and SNB19 cells, which are brain tumor cells). We synthesized the colloidal Au NPs and nanorods according to the procedures in refs 29−32 and coated them with transferrin according to ref 33. For details of all experiments, see Supporting Information. We initially examined the mechanism of cellular uptake. To do this study, we labeled the transferrin protein with the organic fluorophore texas red, adsorbed the fluorescently labeled proteins onto the Au NP surface, and finally, we examined the intracellular uptake of the Au NPs using confocal fluorescence microscopy (see Figure 1). At various *z*-axis, we observed the fluorescently labeled transferrin-coated NPs. If the NPs did not enter cells, we would only observe the fluorescence at the edges of the cells. We demonstrated that three types of cells (HeLa cells, SNB19, and STO cells) took up the NPs, albeit at different concentrations but with similar trends. We refer the interested reader to our previous paper for the quantitation of the cellular uptake of transferrin-coated

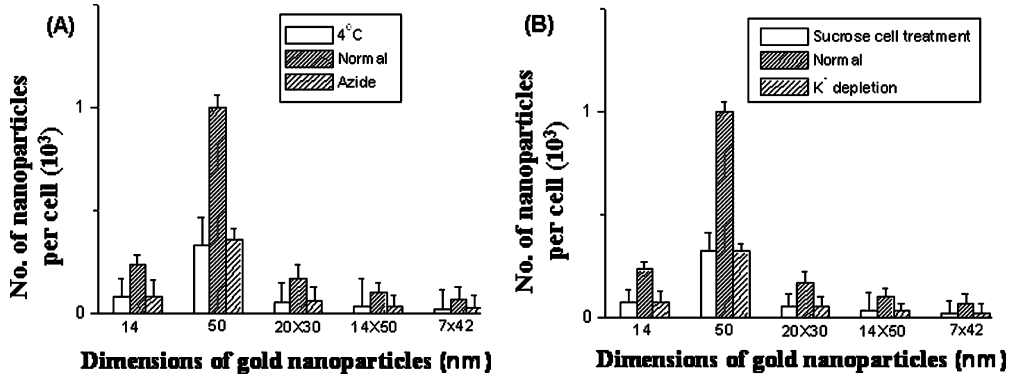

Figure 2. Elucidating the mechanism of transferrin-coated spherical gold nanoparticle and nanorod uptake. (A) This figure shows the uptake of gold nanoparticle and nanorod is dependent upon the receptor-mediated endocytosis pathway. It has been shown that 4 °C and sodium azide treatment can prevent uptake of molecules if it enters the cell via endocytosis. The results also show a large decrease in transferrin-coated gold nanoparticles and nanorods on/in the Hela cell after treatment. (B) This figure shows that the endocytosis pathway is dependent on clathrin. Sucrose and potassium depletion can discrupt the formation of clathrin-coated vesicles.

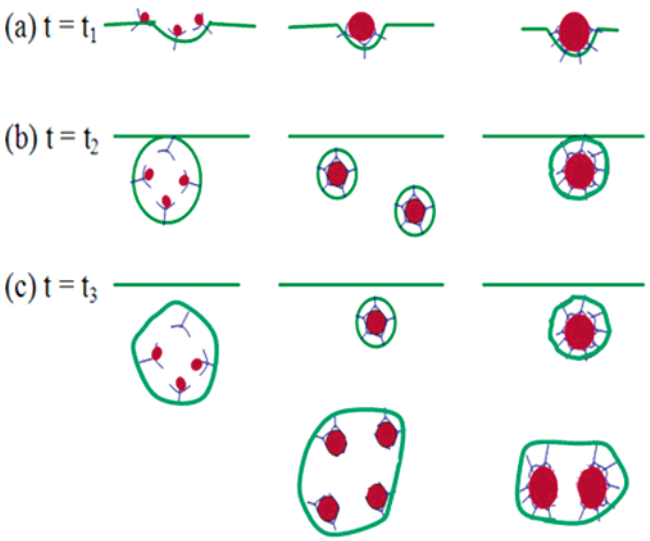

Figure 3. Schematic postulating the size-dependent process of Au NP uptake and fate.

Au NP.[5] Furthermore, we previously demonstrated the uptake of the Au NPs were not toxic to the cells.[5]

We further evaluated the mechanism of uptake of both the spherical versus rod-shaped transferrin-coated NPs. First, we evaluated whether the uptake of the NPs were due to receptor-mediated endocytosis. In these experiments, the NPs were incubated with the cells at either low temperature (4 °C instead of 37 °C) or in ATP-depleted environments (cells pretreated with NaN_3). If the NPs entered via receptor-mediated endocytosis, a decrease in the uptake of the NPs would be observed.[34−36] Indeed, this was the case (∼70% decrease) (see Figure 2A). Next, we determined if uptake was likely due to a clathrin-mediated process. The following studies were done: Cells were pretreated with either sucrose (hypertonic treatment) or a K^+-depleted medium. These conditions are known to disrupt the formation of clathrin-coated vesicles.[35,37,38] These pretreatments showed drastically lower uptake of transferrin-coated Au NPs, and these results indicated that the uptake process was likely due to clathrin-dependence (see Figure 2B). Results were similar for both spherical and rod-shaped NPs, suggesting that the mechanism of uptake was similar. Both Leong and Dai and their co-workers demonstrated that biomolecule-coated carbon nanotubes entered cells via endocytosis,[39,40] suggesting a common

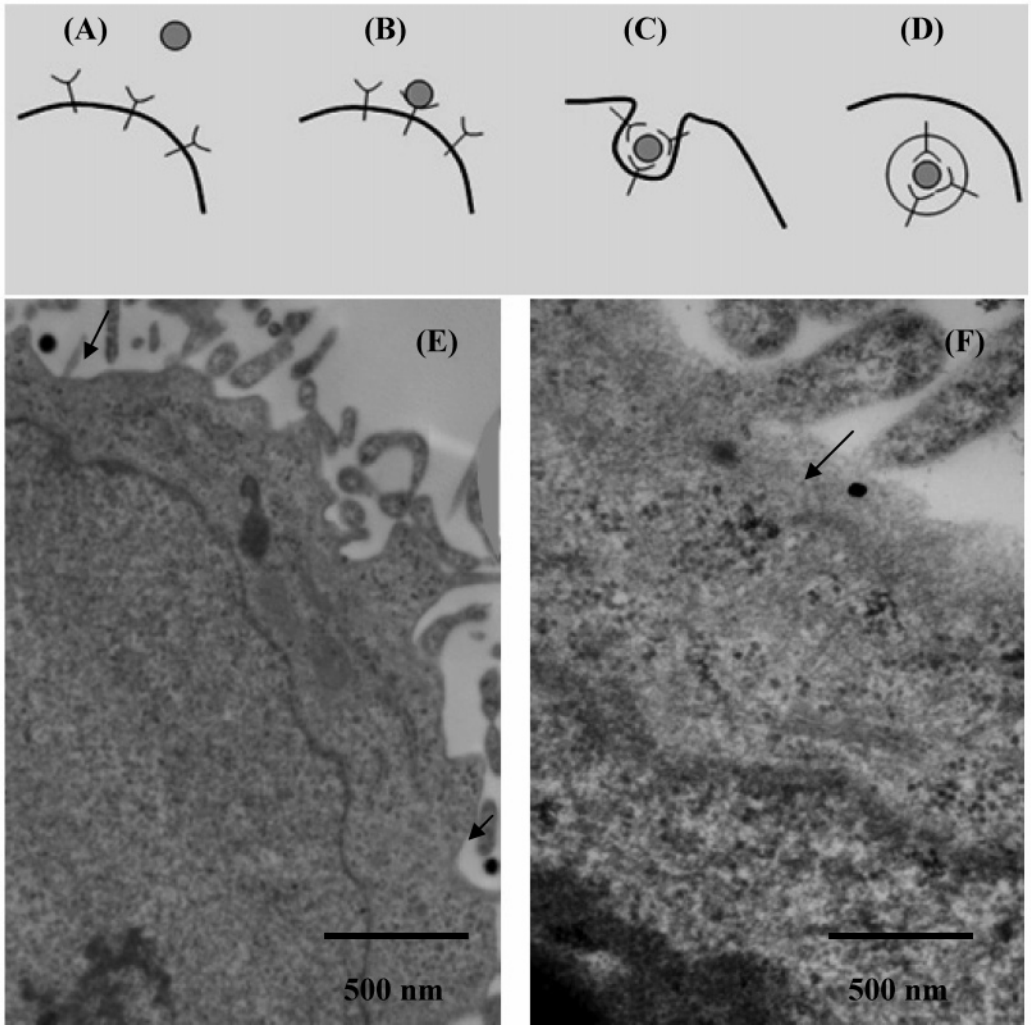

Figure 4. Different stages of the cellular uptake process of ∼50 nm transferrin-coated Au NP. (A−D) Schematic depicting the arrival of a NP at the cell membrane, binding of the nanopartcles to surface receptors, membrane wrapping of the NP, and finally internalization into the cell, respectively. (E−F) TEM images capturing the endocytosis of nanoparticles into Hela cells.

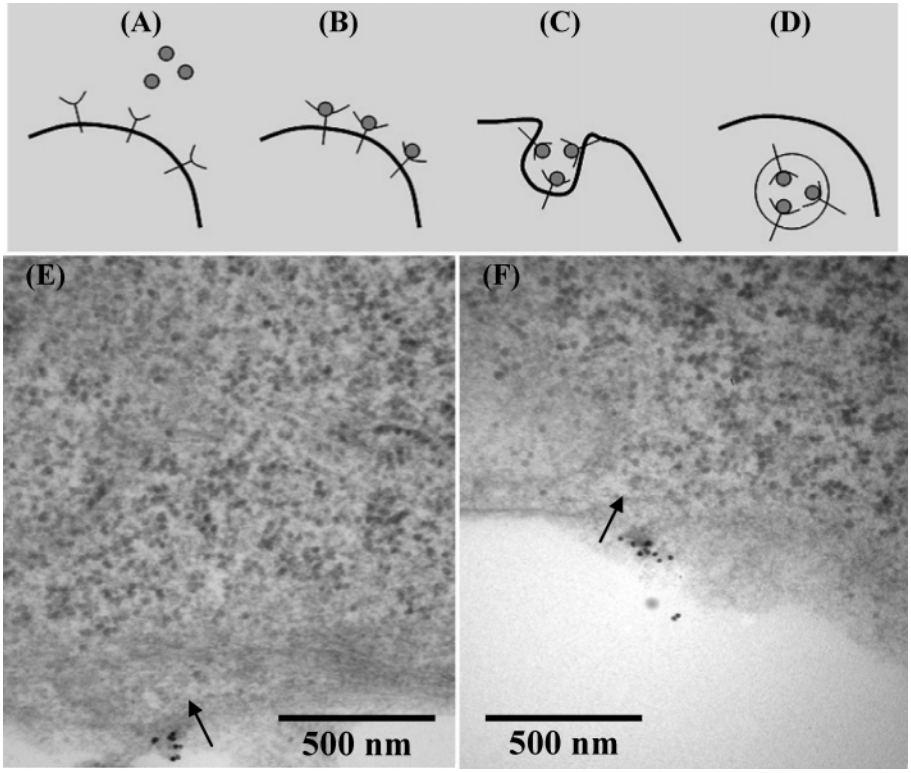

Figure 5. Different stages of the cellular uptake process of ~14 nm transferrin-coated Au NPs. (A−D) Schematic depicting the arrival of a NP at the cell membrane, binding of the nanopartcles to surface receptors, membrane wrapping of the NP, and finally internalization into the cell, respectively. (E−F) TEM images capturing each of these steps. Hela cells were used.

link in uptake mechanism between the different nanoparticles. Other uptake mechanisms could also be possible, but may be to a much lesser extent than endocytosis. In some cases, electron microscopy showed some NPs did not enter cells via an invagination process. In this scheme, a projection from the cell surface reached out and wrapped the NP for uptake (see Supporting Information Figure S1).

We then addressed the question "How does the geometry of Au NPs impact uptake?" A schematic is forwarded to explain the relationship between size of NP and the uptake process (see Figure 3) based on the data and previous studies.[41,42] Many factors, such as ratio of adhesion and membrane stretching, the membrane's bending energy, may be involved in why size affected the uptake of the NPs. These parameters affected the so-called "wrapping time," which described how a membrane enclosed a particle.[43,44] Gao et al. has also suggested that the wrapping time is dependent on particle size.[41,42] The cellular uptake can be considered only as a result of competition between thermodynamic driving force for wrapping and the receptor diffusion kinetics. The thermodynamic driving force refers to the amount of free energy required to drive the NPs into the cell while the receptor diffusion kinetics refer to the kinetics of recruitment of receptors to the binding site. These two factors determined how fast and how many NPs are taken up by the cell. Gao et al. suggested that NPs that were ~55 nm would have the fastest wrapping time and the receptor−ligand interaction can produce enough free energy to drive the NPs into the cell. This minimum wrapping time led to a higher accumulation of the 55 nm NPs into the cell. The docking of a single NP that is smaller than 50 nm will not produce enough free energy to completely wrap the NPs on the surface of the membrane. This could prevent the uptake of the NP by endocytosis. For the smaller NPs to go in, they must be clustered together. For 50 nm, we observed a single NP able to enter the cell, while the 14 nm required at least six NPs to cluster together before uptake (see Figure 4 and 5). For bigger NPs (>50 nm), the wrapping time is slower because of the slower receptor diffusion kinetics (more receptors were taken up during the receptor−ligand binding process and are not available for binding). This led to a smaller number of NPs taken up. Interestingly, in our previous study, we showed that vesicles containing ~50 nm NPs had the highest number per vesicle.[5] Yet, they can enter cells as a single NP. This discrepancy in the results suggests that the vesicle must fuse later on in the cells after entrance. We are currently conducting more studies to understand the activities of the NPs in a cell, and this will be published in a subsequent manuscript.

Next, we characterized the removal of transferrin-coated Au NPs from cells. The removal process (exocytosis) yielded a different trend, as illustrated in Figure 6A. We calculated the fraction of NPs exocytosed (F_{exo}) from the cells by using the following equation:

$$F_{exo} = \frac{N_{OUT}}{N_0} \quad (1)$$

where N_{out} is the number of NPs exocytosed from the cells and N_0 is the number of NPs internalized before exocytosis

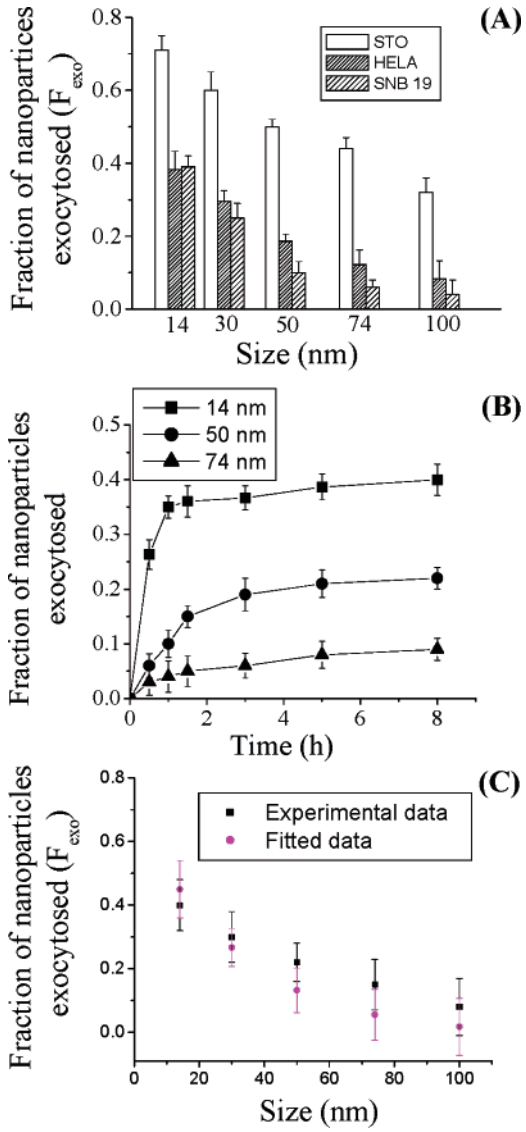

Figure 6. Size dependence of exocytosis of transferrin-coated Au NPs. (A) Size dependence of exocytosis of transferrin-coated Au NPs with sizes between 14 and 100 nm. (B) Kinetics of exocytosis process. (C) Comparison of experimental data with fitted data using eq 2. Hela cells were used to obtain the results in Figure 6B,C.

started. Smaller NPs appeared to exocytose at a faster rate (rate of exocytosis of 14 nm NPs were two times higher than 74 nm NPs) and at a higher percentage than large NPs (e.g., fraction of exocytosis of 14 nm size NPs was five times higher than 100 nm NPs). Dynamics of exocytosis processes are shown in Figure 6B for NPs of sizes 14, 50, and 74 nm. We derived the half-life for the exocytosis process using the data in Figure 6B, where half-life was defined as the time taken to reach half of its equilibrium value. The values of uptake half-life corresponding to exocytosis processes for 14, 50, and 74 nm nanostructures were 0.30, 0.50, and 0.75 h, respectively, for Hela cells, and values corresponding to other cell lines are listed under Supporting Information Figure S2. Interestingly, removal half-life was much faster than the uptake half-life. According to these results, both uptake and removal of NPs were highly dependent upon the size of the NPs but the trends were different.

The same schematic (see Figure 3) used to explain the uptake data can be used to explain the exocytosis results. In this case, the rate of exocytosis of smaller NPs was faster in contrast to larger NPs. This trend occurred in all three cell lines. Smaller NPs will have less receptor−ligand interactions. We speculate that fewer receptor−ligand interactions led to a lower overall binding constant, and hence the transferrin-coated NPs can be released more easily. Previous studies showed that the protein transferrin (not conjugated to anything) exocytosed at a much faster rate than transferrin conjugated to a polymer NP (~2 h longer).[4]

On the basis of our data, we formulated an equation that described the relationship between the fraction of Au NPs exocytosed (F_{exo}) and their size. In this equation, the following factors were considered: (1) Fraction of exocytosis is dependent on the efficiency of dissociation of the receptor−ligand complex on these Au NPs. The number of receptor−ligand complexes was proportional to surface area of each Au NP (S). Hence the rate of exocytosis was inversely proportional to the surface area of the NP. (2) Fraction of Au NPs exocytosed is dependent on the number of NPs internalized in a cell at a given time. (3) Amount of Au NPs endocytosed is negligible if the concentration of NPs in the medium is low.

Hence the fraction of Au NPs exocytosed, F_{exo}, can also be written as follows:

$$F_{exo} = \alpha \frac{N_0}{S} \tag{2}$$

where α is a constant that depends on the cell type and its value is determined experimentally. For the Hela, SNB, and STO cells, the value of α was determined to be 0.3, 0.4, and 1.5, respectively. N_0 is the number of Au NPs internalized at $t = 0$ and S is surface area of each Au NP. $t = 0$ refers to the beginning of the exocytosis process. Figure 6C shows that the fitted data using eq 2 was in close agreement with the experimental data correlating the relationship between sizes of the Au NP with exocytosis. We believe this relationship could be extended to other types of NPs in the sub-100 nm size range and for other protein coatings that enters cells via endocytosis.

Figure 7 illustrates the different stages of the exocytosis process of NPs in cells. NPs about to be removed from cells appeared to be localized in late endosomes and lysosomes (shown as darker contrast in the electron microscopy image and the darker contrast is due to the high electron density of these organelles). TEM images of fixed cells showed the NPs were in many vesicles prior to exocytosis. These vesicles appeared to move toward the cellular membrane (Figure 7A), where they eventually docked (Figure 7B) and released the contents (Figure 7C). The vesicles containing the Au NPs fused with the membrane bilayer, followed by secretion of the NPs into the media. Figure 7D shows TEM images of NPs secreted from the cells. These NPs also contained pieces of lipid bilayer. Previous reports showed membrane lipids were loosened after secretion of contents in vesicles.[45]

On the basis of the exocytosis data, we tried to obtain a "true" quantitation of the endocytosis rates. Data shown in

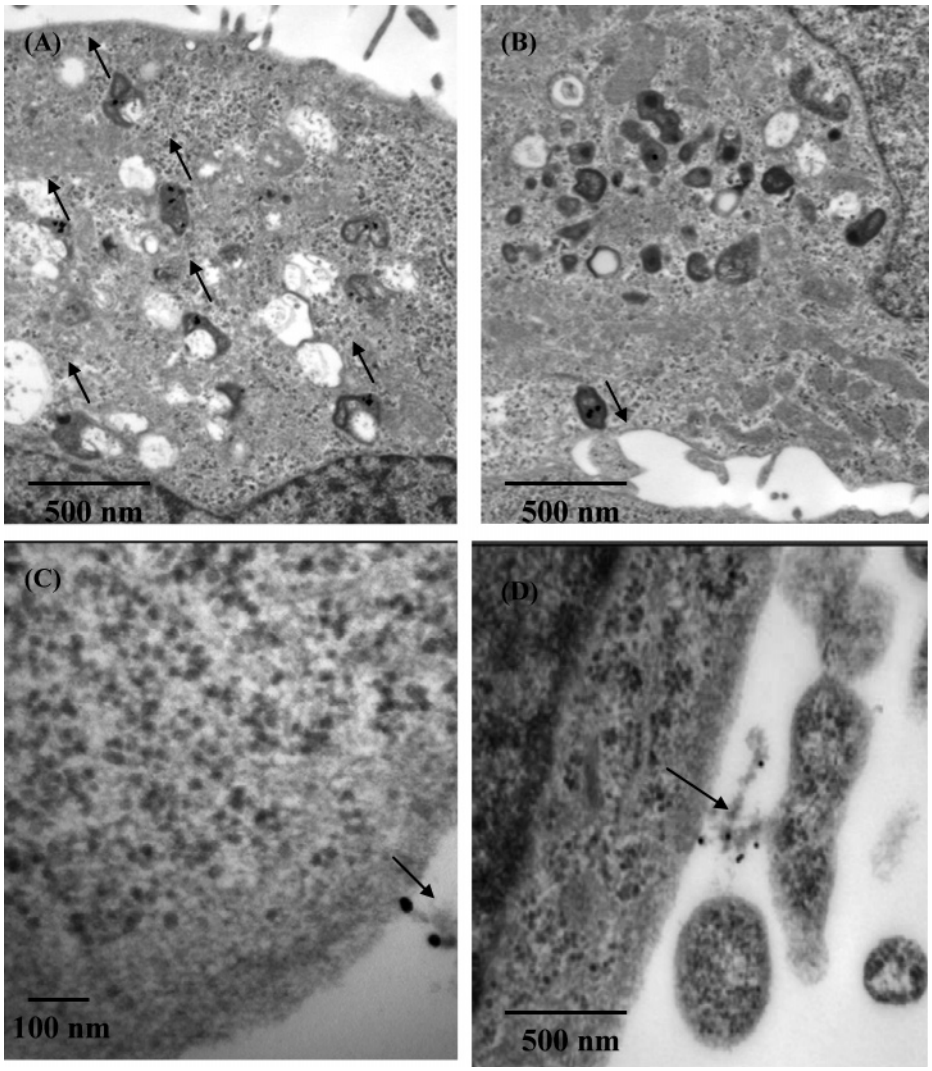

Figure 7. Different stages of the exocytosis process. (A) Movement of the vesicles containing NPs toward the Hela cell membrane. (B) Docking of one of the vesicles at the Hela cell membrane. (C) Excretion of NPs. (D) Cluster of NPs after excretion. Hela cells were used.

ref 5 represents an equilibrium process where removal and uptake of NPs were in dynamics. Hence this data does not provide a real quantitative indicator of only the uptake process. Using the exocytosis data, we attempted to analyze the dependence of size only on the uptake process by decoupling the data from similar experiments obtained for ref 5 using the exocytosis results (Figure 6A,B). The results depicted as Figures 1 and 3 from ref 5 showed the quantitative relationship between size and shape on cellular uptake of uncoated Au NPs. Similar quantitative results were shown with our control experiments (without any transferrin coating). In comparing the transferrin-coated versus uncoated NPs, the data showed a similar trend but a smaller number of NPs locating inside the cell during the uptake and equilibrium process. This smaller uptake concentration could be due to the fact that more than one protein in serum could bind onto the AuNP, providing a higher concentration of Au NPs for uptake as compared to only transferrin protein mediating the uptake. Parts A and B of Figure 8 show the effect of size on the cellular accumulation and kinetics of NPs when exocytosis is considered. This shows a better quantitative dependence of size on uptake. According to Figure 8B, the trend in the dependence of size on uptake did not change. The uptake and removal half-life for NPs with sizes 14, 50, and 74 nm are shown in Figure 8C. Further studies are still needed before a "true" quantitation is determined because, in this study, the uncoated Au NPs can bind onto other proteins in serum, and the mechanism of uptake of all other proteins are not accounted for in this study. Other more complex studies where the exocytosis process is inhibited are needed, and such studies will be a future focus.

Finally, we investigated the impact of shape on uptake and removal. Rod-shaped NPs such as carbon nanotubes and Au nanorods have recently been explored as potential candidates for molecular transporters and thermal therapy.[39,40,46] We have also evaluated how shape of NPs impacted its uptake and release mechanisms. The TEM image and optical absorption spectra of nanorods used for the experiments are given in Supporting Information Figure S3. See Figure 9 and Supporting Information Figure S4 for representative TEM images of the uptake, residence, and release of the rod-shaped NPs. On the basis of Figure 9A, it appeared that the uptake of transferrin-coated rod-shaped NPs

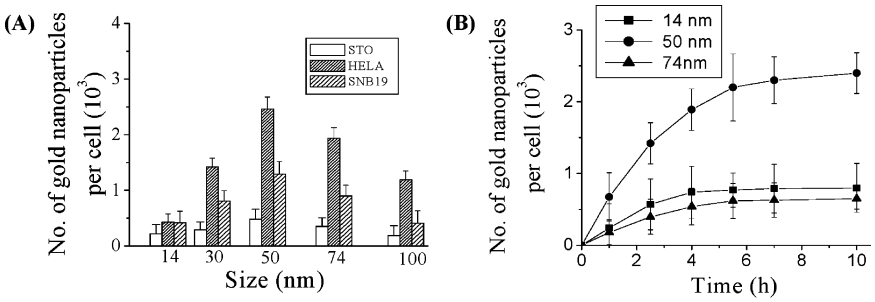

(C)

Size of the nanoparticles	Hela		SNB19		STO	
	Uptake Half-life (hrs)	Removal Half-life (min)	Uptake Half-life (hrs)	Removal Half-life (min)	Uptake Half-life (hrs)	Removal Half-life (min)
14 nm	1.19	0.33	2.02	0.41	2.45	0.33
50 nm	1.71	0.50	1.88	0.58	2.10	0.41
74 nm	2.12	0.75	2.52	0.66	2.88	0.58

Figure 8. Size dependence of uptake after decoupling equilibria data from Figure 1B. Decoupling refers to the subtraction of equilibrium data from exocytosis data. This leads to a more accurate indicator of NP uptake concentration and rate. (A) Size dependence on uptake process. (B) Kinetics of the uptake process for Hela cells. (C) Table consists of Hela cell uptake and removal half-life corresponding to transferrin-coated Au NPs with sizes 14, 50, and 74 nm.

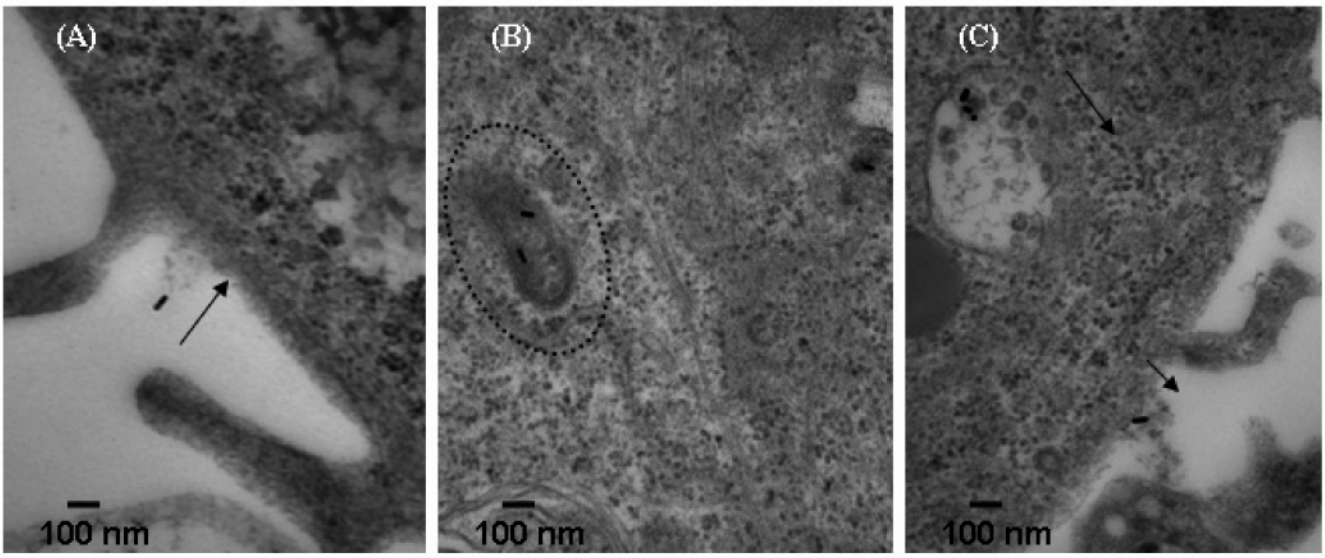

Figure 9. Different stages of the cellular uptake, residence, and removal of transferrin-coated Au nanorods. (A) Attachment of the nanorod onto the Hela cell membrane. (B) Localization of the nanorods in the endosomal vesicles. (C) Excretion of nanorods from cell membrane. Hela cells were used. More images are shown in Supporting Information Figure S4.

was much less than transferrin-coated spherical NPs. The uptake data were obtained by subtracting the equilibria data from the exocytosis data (similar to the spherical Au NP). To illustrate, the 50 nm × 50 nm transferrin-coated Au NPs took up ~5−7 times more NPs (depending on the cell line). With these studies, the uptake of the rod-shaped NPs appeared to be more dependent upon the width of the NP in comparison to the length (by comparing the data in Figure 10A from the different rod-shaped NPs). We speculated that the position of the transferrin on the Au nanorods played a significant role in the uptake process. Although it is currently difficult to measure the location of the transferrin protein on the surface of the nanorods, we speculated that the transferrin protein was only bound to the ends of the nanorods based on previous studies by Murphy et al.[47] and Tan et al.[48] They demonstrated that proteins were only adsorbed onto the ends of the Au nanorods because the surface-stabilizing molecule CTAB was difficult to remove in the longitudinal direction. Both groups showed that adsorption of the protein avidin on the Au nanorods led to end-to-end assembly of the nanorods when biotinylated molecules were introduced. The TEM image of nanorod uptake also showed the end of the transferrin-coated nanorods binding to the cell membrane (see Figure 9A). We also speculated that the low amounts of nanorod uptake is related to the wrapping time, where it took longer to wrap the entire

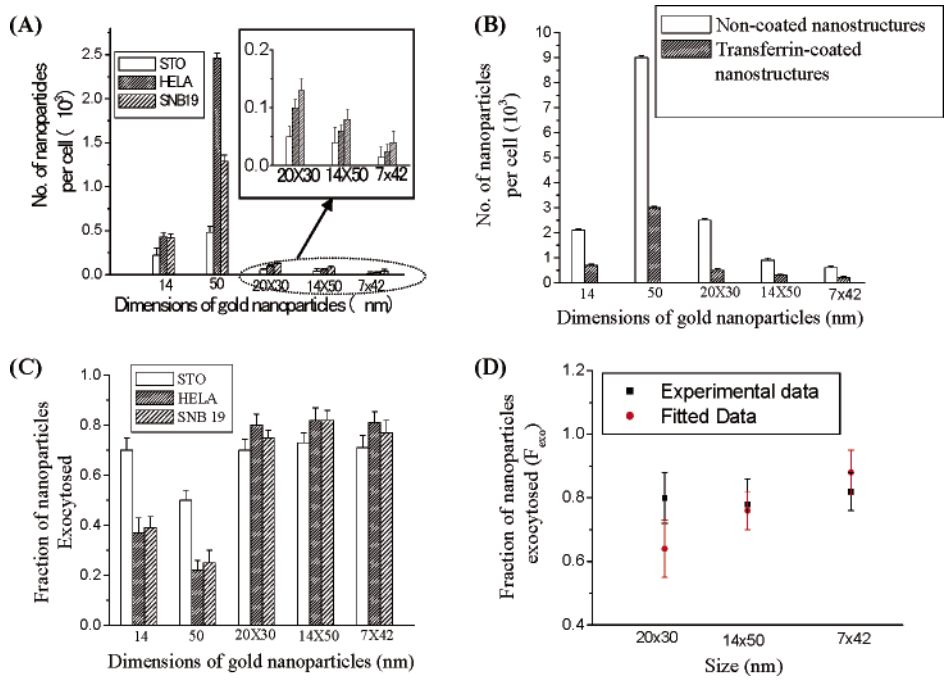

Figure 10. Comparison of uptake and removal of transferrin-coated spherical Au NPs versus Au nanorods. (A) Uptake data (after decoupling) demonstrates that lower concentration of transferrin-coated Au nanorods uptake in comparison to their spherical counterpart. (B) The uptake of uncoated spherical Au NPs and nanorods. (C) The fraction of exocytosis of transferrin-coated Au NPs and nanorods. (D) Comparison of data obtained from the fraction of exocytosis of transferrin-coated Au nanorods vs that of fitted data obtained from eq 2. Hela cells were used to obtain the results in Figure 10 B,C.

rod in comparison to the sphere because of the increase in the surface area. Of note, similar to the spherical-shaped Au NP, the transferrin-coated nanorods showed a lower uptake in comparison to the uncoated nanorods (Figure 10B).

We also observed a large difference (with the exception of STO cells) between the percentages of exocytosis of transferrin-coated nanorods versus spherical-shaped NPs (see Figure 10C). The protein transferrin is likely coated on the ends of the nanorods. With such a scenario, the fitting of the exocytosis data by eq 2 could predict the fraction of rod-shaped NP exocytosed in a fashion similar to the spherical shaped NPs. Indeed, for the 14 nm × 50 nm and 7 nm × 42 nm transferrin-coated nanorod, there was a close correlation between the fraction of Au nanorod exocytosed with that of the 14 and 7 nm transferrin-coated spherical NPs (see Figure 10D). However, we observed a larger deviation from the 20 nm × 30 nm transferrin-coated nanorod versus 20 nm transferrin-coated spherical NP. In contrast to the larger aspect ratio nanorods, the percentage of surface coverage of the transferrin on the 20 nm × 30 nm should be much greater than the 14 nm × 50 nm and 7 nm × 42 nm nanorods because the lower aspect ratio nanorods have greater surface curvature at the ends of the nanorod (this could possibly lead to greater binding strength of the transferrin-coated nanorod to the receptors on the cell surface and hence affects the exocytose rates). Of note, these results suggest that it is difficult to fit the data into eq 2 for assessing exocytosis when the nanorods have aspect ratios of 1.1−2.0.

In this work, we investigated why the cellular uptake of NPs was related to size and shape. Initially, we showed that the transferrin-coated NPs were taken up into the cells via a receptor-mediated clathrin-dependent endocytosis pathway. We proposed the concept of particle "wrapping time," which explained why NPs of different sizes and shapes affected uptake rate. We also demonstrated the removal of the transferrin-coated NPs was linearly related to size, which was different than the uptake process. Last, using the removal data, we obtained a more accurate quantitation of NP endocytosis as it related to size. Furthermore, rod-shaped NPs showed a lower uptake in comparison to spherical shaped nanoparticles. The rates of uptake were lower with an increasing aspect ratio. The fraction of rod-shaped NPs exocytosed was higher than spherical-shaped nanostructures. These studies show that the selection of the NPs can influence the accumulation concentration and rates of the NPs in a cell. The optimization of such parameters will lead to improvements in the design of smart NP carriers for various biomedical applications.

Acknowledgment. WCWC acknowledges CIHR, NSERC, CFI, OIT, and University of Toronto for financial support. D.B. would like to thank NSERC for fellowship. We would like to acknowledge Dan Mathers and Ying Lee at Analyst Laboratory and Battista Cavieri at TEM facility for technical assistance.

Supporting Information Available: Materials and methods; additional data. This material is available free of charge via the Internet at http://pubs.acs.org.

References

(1) Klostranec, J. M.; Chan, W. C. W. *Adv. Mater.* **2006**, *18*, 1953.
(2) Hong, R.; Han, G.; Fernandez, J. M.; Kim, B.-J.; Forbes, N. S.; Rotello, V. M. *J. Am. Chem. Soc.* **2006**, *128*, 1078.

(3) Derfus, A. M.; Chan, W. C. W.; Bhatia, S. N. *Adv. Mater.* **2004**, *16*, 961.
(4) Sahoo, S. K.; Labhasetwar, V. *Mol. Pharmaceutics* **2005**, *2*, 373.
(5) Chithrani, B. D.; Ghazani, A. A.; Chan, W. C. W. *Nano Lett.* **2006**, *6*, 662.
(6) Xu, X. H. N.; Brownlow, W. J.; Kyriacou, S. V.; Wan, Q.; Viola, J. J. *Biochemistry* **2004**, *43*, 10400.
(7) Fischer, H.; Li, L.; Pang, K. S.; Chan, W. C. W. *Adv. Funct. Mater.* **2006**, 1*6*, 1299.
(8) Osaki, F.; Kanamori, T.; Sando, S.; Sera, T.; Aoyama, Y. *J. Am. Chem. Soc.* **2004**, *126*, 6520.
(9) Nakai, T.; Kanamori, T.; Sando, S.; Aoyama, Y. *J. Am. Chem. Soc.* **2003**, *125*, 8465.
(10) Rensen, P. C. N.; Sliedregt, L. A. J. M.; Ferns, M.; Kieviet, E.; Ressenberg, S. M. W. V.; Leeumen, S. H. V.; Berkel, T. J. C. V.; Biessen, E. A. L. *J. Biol. Chem.* **2001**, 276, 37577.
(11) Champion, J. A.; Mitragotri, S. *Proc. Natl. Acad. Sci. U.S.A.* **2006**, *103*, 4930.
(12) Sheff, D.; Pelletier, L.; O'Connel, C. B.; Warren, G.; Mellmann, I. *J. Cell Biol.* **2002**, *156*, 797.
(13) Jiang, W.; Singhal, A.; Zheng, J.; Wang, C.; Chan, W. C. W. *Chem. Mater.* **2006**, *18*, 4845.
(14) Li, H.; Sun, H. Qian, Z. M. *Trends Pharm. Res.* **2002**, *23*, 206.
(15) Dautry-Varsat, A.; Ciechanover, A.; Lodish, H. F. *Proc. Natl. Acad. Sci. U.S.A.* **1983**, *80*, 2258.
(16) Quan, Z. M.; Li, H.; Sun, H.; Ho, K. *Pharmocol. Rev.* **2002**, *54*, 561.
(17) Widera, A.; Norouzyan, F.; Chen, W. C. *Adv. Drug Delivery* **2003**, *55*, 1439.
(18) Yang, P. H.; Sun, X.; Chiu, J. F.; Sun, H.; He, Q. Y. *Bioconjugate Chem.* **2005**, *16*, 494.
(19) Wagner, E.; Zatloukal, K.; Cotten, M.; Kiriappos, H.; Mechtler, K.; Curiel, D. T.; Birnstiel, M. L. *Proc. Natl. Acad. Sci. U.S.A.* **1992**, *89*, 6099.
(20) West, J.; Halas, N. J. *Annu. Rev. Biomed. Eng.* **2003**, 5, 285.
(21) Paciotti, G. F.; L. Myer, Weinreich, D.; Goia, D.; Pavel, N.; McLaughlin, R. E.; Tamarkin, L. *Drug Delivery* **2004**, *11*, 169.
(22) Jiang, W.; Papa, E.; Fischer, H.; Mardyani, S.; Chan, W. C. W. *Trends Biotechnol.* **2004**, *22*, 607.
(23) Alivisatos, A. *Nat. Biotechnol.* **2004**, *22*, 47.
(24) Wu, X.; Liu, H.; Liu, J.; Haloy, K. N.; Treadway, J. A.; Larson, J. P.; Ge, N.; Peale, F.; Bruchez, M. P. *Nat. Biotechnol.* **2003**, *21*, 41.
(25) Chan, W. C. W.; Maxwell, D. J.; Gao, X.; Bailey, R. E.; Han, M.; Nie, S. *Curr. Opin. Biotechnol.* **2002**, *13*, 40.
(26) Loo, C.; Lowery, A.; Halas, N.; West, J.; Drezek, R. *Nano Lett.* **2005**, *5*, 709.
(27) Huang, X.; El-Sayed, I. H.; Qian, W.; El-Sayed, M. A. *J. Am. Chem. Soc.* **2006**, *128*, 2115.
(28) Hirsch, L. R.; Stafford, R. J.; Bankson, J. A.; Sershen, S. R.; Rivera, B.; Rrice, R. E.; Hazle, J. D.; Halas, N. J.; West, J. *Proc. Natl. Acad. Sci. U.S.A.* **2003**, *100*, 13549.
(29) Frens, G. *Phys. Sci.* **1973**, *241*, 20.
(30) Freeman, R. G.; Grabar, K. C.; Allison, K. J.; Bright, R. M.; Davis, J. A.; Guthrie, A. P.; Hommer, M. B.; Jackson, M. A.; Smith, P. C.; Walter, D. G.; Nathan, M. J. *Science* **1995**, *267*, 1629.
(31) Nikoobakht, B.; El-Sayed, M. *Langmuir* **2003**, *15*, 1957.
(32) Sau, T. P.; Murphy, C. J. *Langmuir* **2004**, *20*, 6414.
(33) Hermanson, G. T. *Bioconjugate Techniques*; Academic Press: New York, 1996.
(34) Schmid, S. L.; Carter, L. L. *J. Cell Biol.* **1990**, *111*, 2307.
(35) Kam, N. W. S.; Liu, Z.; Dai, H. *Nanotechnology* **2006**, *45*, 577−581.
(36) Silverstein, S. C.; Steinman, R. M.; Cohn, Z. A. *Annu. Rev. Biochem.* **1977**, *46*, 669.
(37) Daukas, G.; Zigmond, S. H. *J. Cell Biol.* **1985**, *101*, 1673.
(38) Larkin, J. M.; Brown, M. S.; Austein, J. L.; Anderson, R. G. W. *Cell* **1983**, *33*, 273.
(39) Liu, Y.; Wu, D.-C.; Zhang, W.-D.; Jiang, X.; He, T. S.; Goh, S. H.; Leong, K. W. *Angew. Chem., Int. Ed.* **2005**, *44*, 4782.
(40) Kam, N. W. S.; Liu, Z.; Dai, H. *Angew. Chem., Int. Ed.* **2006**, *45*, 577.
(41) Gao, H.; Shi, W.; Freund, L. B. *Proc. Natl. Acad. Sci. U.S.A.* **2005**, *102*, 9469.
(42) Bao, G.; Bao, X. R. *Proc. Natl. Acad. Sci. U.S.A.* **2005**, 9997.
(43) Tzlil, S.; Desermo, M.; Gelbart, W. M.; Ben-Shaul, A. *Biophys. J.* **2004**, *86*, 2037.
(44) Deserno, M.; Gelbart, W. M. *J. Phys. Chem. B* **2002**, *106*, 5543.
(45) Taraska, J. W.; Almers, W. *Proc. Natl. Acad. Sci. U.S.A.* **2004**, *101*, 8780.
(46) Pantarotto, D.; Singh, R.; McCarthy, D.; Erhardt, M.; Briand, J.; Prato, M.; Kostarelos, K.; Bianco, A. *Angew. Chem., Int. Ed.* **2004**, *43*, 5242.
(47) Caswell, K. K.; Wilson, J. N.; Bunz, U. H. F.; Murphy, C. J. *J. Am. Chem. Soc.* **2003**, *125*, 13914.
(48) Chang, J. Y.; Wu, H.; Chen, H.; Ling, Y. C.; Tan, W. *Chem. Commun.* **2005**, 1092.

NL070363Y